Colloid Polym Sci (2017) 295:1491–1498
DOI 10.1007/s00396-017-4131-8

ORIGINAL CONTRIBUTION

Dispersion of hydroxyapatite nanocrystals stabilized by polymeric molecules bearing carboxy and sulfo groups

Kazuya Watanabe[1] · **Ikuko Nishida**[1] · **Hiroaki Imai**[2]

Received: 19 March 2017 / Revised: 5 June 2017 / Accepted: 12 June 2017 / Published online: 22 June 2017

Abstract Calcium phosphate buildup is important for biological processes (e.g., bones and teeth growth) and negatively affects the efficiency and functioning of water systems (e.g., cooling water systems and boilers) as a result of scale buildup by salts precipitation. Thus, stable aqueous dispersions of calcium phosphate particles can effectively prevent the formation and buildup of scale in water systems. In this study, the stabilization of calcium phosphate nanocrystals (NCs) was studied by forming a supersaturated solution in the presence of poly acrylic acid/2-acrylamide-2-methylpropane sulfonic acid p(AA/AMPS) containing carboxy and sulfo group functionalities. Calcium phosphate NCs were formed and subsequently aggregated in a supersaturated aqueous solution containing 2-phosphonobutane-1,2,4-tricarboxylic acid without any copolymers. Aggregation of calcium phosphate NCs was suppressed in the presence of polymeric molecules containing carboxy groups, whereas molecules bearing sulfo groups were ineffective in dispersing calcium phosphate NCs. However, copolymers bearing both functional groups enhanced the dispersibility of calcium phosphate NCs. Using a combination of light scattering and surface charge measurements along with electron imaging, we found that the inhibition of calcium phosphate precipitation originates from hydroxyapatite nanocrystals (HANCs) with a size smaller than 100 nm in solution. While the carboxy groups in the copolymer adsorbed on the surface of the HANCs, the sulfo groups provided these species with an overall negative surface charge, thereby increasing their colloidal stability via electrostatic repulsion. These results indicated that the aggregation of the HANCs can be effectively hindered using sulfo/carboxy bifunctional copolymers.

Keywords Dispersibility · Hydroxyapatite · Nanocrystals · Inhibition ability · Sulfo groups · Surface negativity

✉ Kazuya Watanabe
kazuya.watanabe@kurita.co.jp

Ikuko Nishida
ikuko.nishida@kurita.co.jp

Hiroaki Imai
hiroaki@applc.keio.ac.jp

[1] Kurita Water Industries Ltd., 1-1, Kawada, Nogi-machi, Shimotsuga-gun 329-0105, Japan

[2] Department of Applied Chemistry, Faculty of Science and Technology, Keio University, 3-14-1 Hiyoshi, Kohoku-ku, Yokohama 223-8522, Japan

Introduction

Scale formation via precipitation of calcium carbonate and calcium phosphate on the surface of high-temperature heat exchangers is a persistent problem in cooling water systems [1, 2]. Scale deposits cause a number of issues such as obstruction of fluid flow, heat transfer impedance, wear of metal parts, localized corrosion attack, and unscheduled equipment shutdown [3]. These issues have motivated the development of calcium carbonate and calcium phosphate scale inhibitors containing acrylic acid (AA)-based polymers and phosphonic acid that adsorb on the growth sites of submicroscopic crystallites [1, 3–7]. Previous studies have shown that AA-based polymers containing sulfo groups effectively inhibit calcium phosphate scale formation. In this sense, Amjad et al. demonstrated that a copolymer of AA and 2-acrylamide-2-methylpropane sulfonic acid (AMPS) p(AA/AMPS) is more effective in inhibiting calcium phosphate scale formation as compared with separate p(AA) or p(AMPS) homopolymers [1, 2, 8]. Moreover, Amjad et al. evaluated the hydroxyapatite

(HA) dispersion by polymers containing carboxy and sulfo groups/phosphonate blends. However, the mechanism of HA dispersion by polymer/phosphonate blends is not clear [9].

Interactions between biomimetic polymers and calcium phosphate crystals have become important in fields such as biomineralization of bones and teeth. Thus, the formation process and properties of calcium phosphate have been controlled upon studying its interaction with functionalized polymers [10–23]. In particular, several studies have examined the interactions between carboxy functional groups and calcium phosphate. Shen et al. demonstrated that carboxy groups adsorb on the surface of HA (a common mineral form of calcium phosphate) after nucleation [18]. Ofir et al. found that polyglutamic acids having carboxy groups adsorb on the surface of amorphous calcium phosphate (ACP), thereby negatively charging the ACP [20]. However, for polymers having only carboxy groups, Daniel et al. proposed that excess divalent calcium ions may bind to the carboxy groups in polymers and decrease their electrostatic repulsion to physically crosslink the polymers [21]. The stabilization of calcium phosphate particles by negative charging is very important to effectively prevent scale formation. Therefore, the inhibition mechanism of calcium phosphate precipitation by p(AA/AMPS) having not only carboxy groups but also sulfo groups must be elucidated for more effective prevention of scale formation. Furthermore, in scale inhibition studies for cooling water systems, the effect of macroscopic particles larger than 100 nm in size is typically examined, and calcium phosphate particles with smaller sizes are neglected [1, 8]. In the present study, we focused on the colloidal stability of small calcium phosphate particles (smaller than 100 nm) by examining their size, surface charge, and aggregation behavior in solution as well as their surface interaction with various homo- and copolymers. We found that the carboxy groups of p(AA/AMPS) anchored onto the surface of calcium phosphate, whereas the sulfo groups provided negative charge to these species, thus promoting stable dispersion in an aqueous solution.

Experimental

Materials

AA and AMPS were purchased from Sigma-Aldrich Co. All other reagents including calcium salts were purchased either from Kishida Chemical Co. Ltd. or Bayer AG and used as received.

Free radical polymerization of p(AA), p(AMPS), and p(AA/AMPS)

P(AA), p(AMPS), and p(AA/AMPS) were synthesized by free radical polymerization in an aqueous solution at 60 °C with ammonium persulfate as the initiator. A series of p(AA/AMPS) was synthesized by controlling the AA:AMPS molar ratio. The relative molecular weights were measured by size exclusion chromatography calibrated with sodium polyacrylate standards (M_w = 6300–9600 g mol^{-1}).

Calcium phosphate precipitation experiments

Calcium carbonate and calcium phosphate are the most frequently encountered deposits in cooling water systems [24]. 2-phosphonobutane-1,2,4-tricarboxylic acid (PBTC) is typically used as a stabilizing agent for calcium carbonate in cooling water systems [4]. Thus, addition of PBTC significantly influenced the calcium carbonate crystal growth kinetics via adsorption on the surface of calcium carbonate and subsequent suppression of the precipitation process [4]. Herein, the ability of AA-based polymers (Fig. 1) for avoiding calcium phosphate precipitation in aqueous solutions was believed to follow a similar mechanism.

Supersaturated calcium phosphate test solutions were prepared by diluting the following stock solutions in pure water in the given order. PBTC (3.7 mmol dm^{-3}), Na_2HPO_4 (17.6 mmol dm^{-3}), $NaHCO_3$ (25 mmol dm^{-3}), and $CaCl_2$ (250 mmol dm^{-3}) were diluted to obtain final concentrations of Ca^{2+}, PO_4^{3-}, HCO_3^-, and PBTC of 1, 0.16, 2, and 0.005 mmol dm^{-3}, respectively. Calcium phosphate precipitation was studied in the presence of AA-based polymers, which were added to the above test solution before the addition of the $CaCl_2$ solutions. A number of AA-based polymers (i.e., no polymer, p(AA), p(AMPS), and p(AA/AMPS)) with varying AA:AMPS molar ratios ([AA]:[AMPS] = 97:3, 89:11, 85:15, 74:26, 66:34, 48:52, 43:57, 29:71, 24:76, and 13:87) were tested. Subsequently, the pH was adjusted to 8.5 using HCl

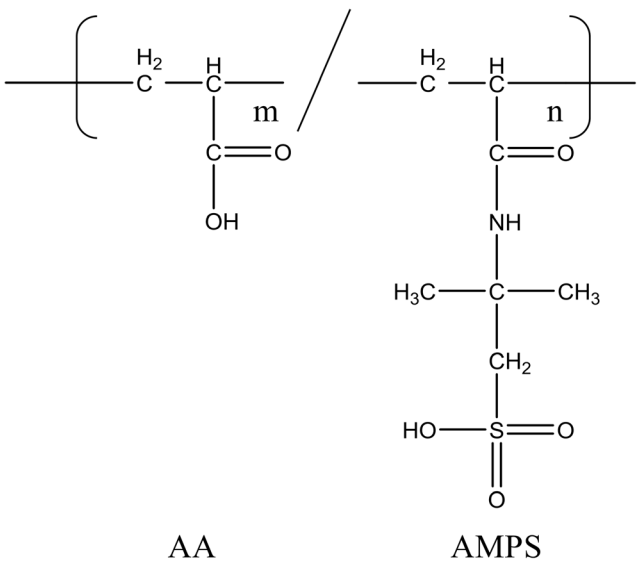

Fig. 1 Chemical structure of acrylic acid (AA)-based polymers

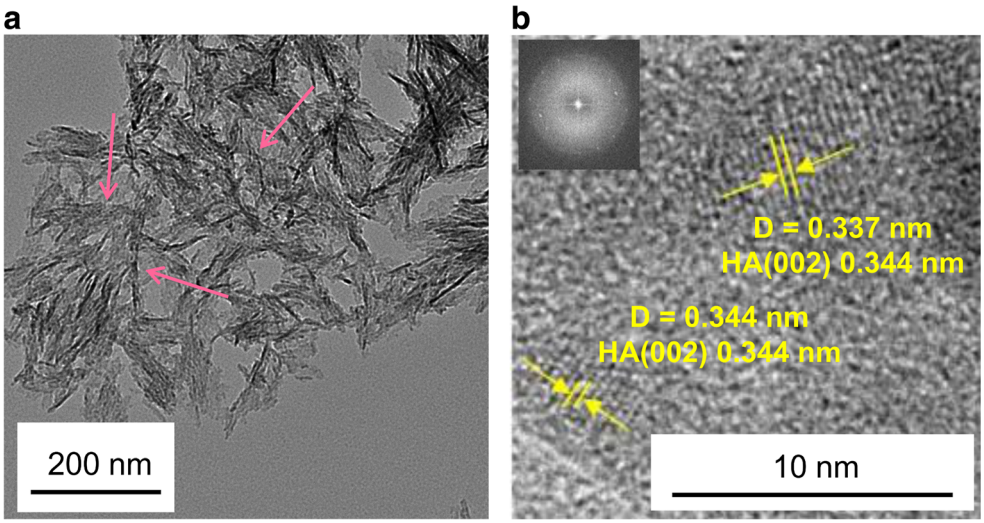

Fig. 2 Transmission electron microscopy (TEM) images of calcium phosphate particles formed in the absence of polymers in a supersaturated solution. Inset in (**b**) shows the Fourier transform of the image. The *arrows* indicate the rod-shaped particles of approximately 200 nm length and 10 nm width

and NaOH. The supersaturated calcium phosphate solutions were then placed in a water bath at 60 °C for 20 h, and precipitation was monitored by analyzing the phosphate concentration in aliquots of the filtered solution (pore size: 100 nm, Millipore, VVLP01300) using a standard colorimetric method [1, 8]. Precipitation of calcium phosphate was considered to start when the calcium phosphate particles grew to sizes larger than 100 nm.

Instrumental analysis

The sizes of the calcium phosphate particles formed in the solutions after 20 h were measured via dynamic light scattering (DLS, Malvern Zetasizer Nano) and laser scattering (LS, Shimadzu SALD-7000) without filtration. The solutions were observed by transmission electron microscopy (TEM, FEI Tecnai F20). To prepare the TEM samples, the solutions were stood for 20 h, and a drop of each solution was subsequently placed onto copper grids and dried at room temperature before filtration. The zeta potential of the particles in the solution was measured at 60 °C using a Malvern Zetasizer Nano system.

Results

Precipitation of calcium phosphate in a supersaturated solution

Figure 2 shows TEM images of the calcium phosphate particles formed without any polymers and in the presence of

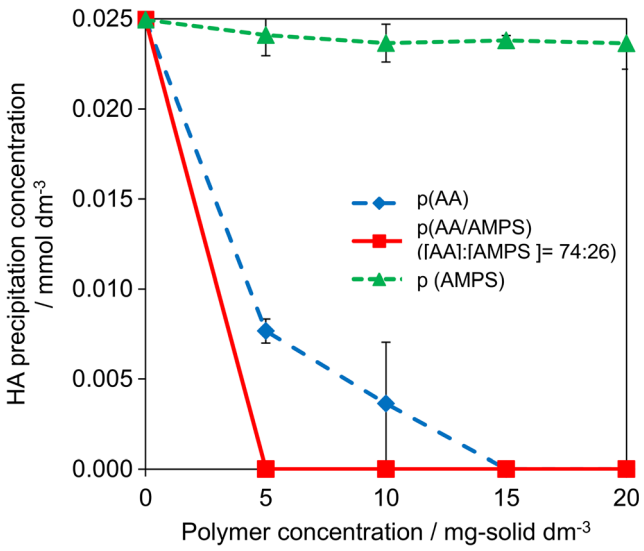

Fig. 3 Hydroxyapatite (HA) precipitation concentration as a function of polymer concentration. *Error bars* show the mean standard deviation after three determinations. No error bars indicate zero or very low standard deviation

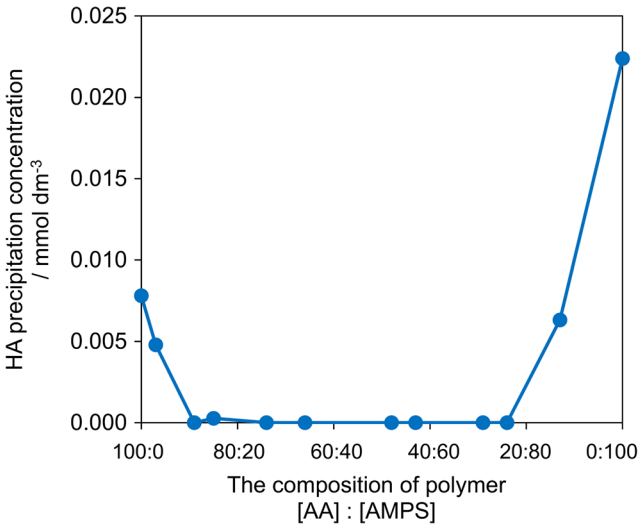

Fig. 4 HA precipitation concentration with poly acrylic acid/2-acrylamide-2-methylpropane sulfonic acid p(AA/AMPS)) copolymers as a function of the AA:AMPS molar ratio. The polymer composition refers to the AA to AMPS molar ratio. The overall polymer concentration was 5 mg dm^{-3}. This data were measured only one time

PBTC in a supersaturated calcium phosphate solution. Microscale aggregates comprising rod-shaped nanocrystals (NCs) of approximately 200 nm length and 10 nm width (Fig. 2a) were observed. As shown in Fig. 2b, the 0.344 nm lattice spacing observed in the high-resolution TEM image was assigned to the (002) plane of HA [25].

Inhibition of calcium phosphate precipitation by polymers

Figure 3 shows the relation between the polymer concentration and the concentration of hydroxyapatite nanocrystals (HANC) precipitates (polymers employed: p(AA), p(AA/AMPS) with [AA]:[AAMPS] = 74:26, and p(AMPS)). HANCs aggregation was slightly suppressed by p(AMPS) regardless of the polymer concentration. On the other hand, p(AA) completely inhibited HANC precipitation at polymer concentrations above 15 mg dm^{-3}. Precipitation was not observed in the presence of p(AA/AMPS) at concentrations greater than 5 mg dm^{-3}.

We examined the precipitation of HANCs in the presence of p(AA/AMPS) copolymers while varying the AA:AMPS molar ratio (Fig. 4, overall polymer concentration fixed at 5 mg dm^{-3}). HANCs precipitation was completely suppressed at [AA]:[AMPS] ratios ranging from 89:11 to 24:76. These results suggest that the combination of carboxy and sulfo groups was highly effective for inhibiting phosphate precipitation.

We determined the size of the particles formed in solutions containing polymers such as p(AA), p(AA/AMPS), ([AA]:[AAMPS] = 74:26), and p(AMPS) via DLS and LS measurements (Fig. 5). At p(AA) and p(AA/AMPS) polymer concentrations exceeding 5 and 15 mg dm^{-3}, respectively, the particles remained dispersed in the solution. The size of the particles dispersed in the solution containing p(AA) and p(AA/AMPS) was smaller than 100 nm. Therefore, the tested polymers inhibited calcium phosphate precipitation by limiting the growth of the HANCs below 100 nm in size. Moreover, the solution containing p(AA/AMPS) formed particles with smaller size as compared to p(AA) (8 vs. 37 nm). These smaller particles were stabilized by p(AA/AMPS), which showed high inhibition ability for calcium phosphate precipitation.

Figure 6 shows the relation between the polymer concentration and the zeta potential of the particles in solution. The zeta potential of the HANCs generated without polymers was almost zero, and this value decreased with the polymer concentration for HANCs formed in the presence of p(AA) and p(AA/AMPS) ([AA]:[AMPS] = 76:24). Thus, these results indicated that polymers inhibited precipitation by increasing the negative surface charge of HANCs. Remarkably, the zeta potential was not affected by the addition of p(AMPS). These results clearly showed that HANC precipitation was inhibited when these species were negatively charged in solution.

Morphological variation of calcium phosphate by the polymers

Figures 7, 8, and 9 show TEM images of the HANCs formed in the presence of p(AA), p(AA/AMPS) ([AA]:[AAMPS] = 74:26), and p(AMPS), respectively, at a polymer concentration of 20 mg dm^{-3}. As shown in Fig. 7a, b, aggregates of rod-shaped particles of approximately 200 nm were obtained in the presence

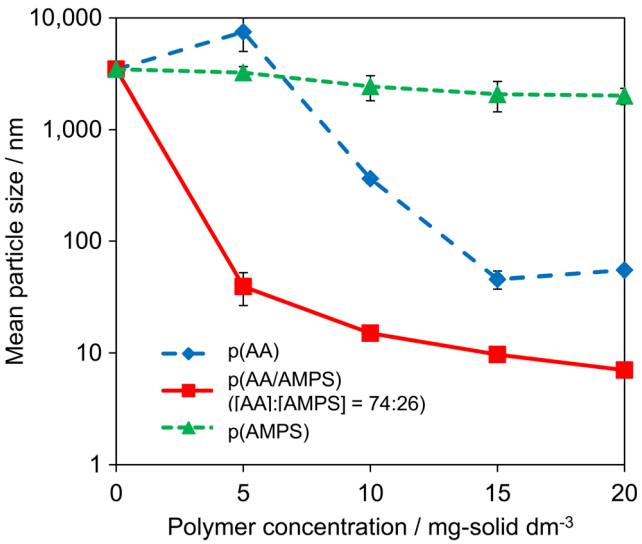

Fig. 5 Mean particle size measured by DLS and LS. Particles larger than 1000 nm in size were measured by LS. Particles smaller than 1000 nm in size were measured by DLS. *Error bars* show the mean standard deviation after three determinations. No error bars indicate zero or very low mean standard deviation

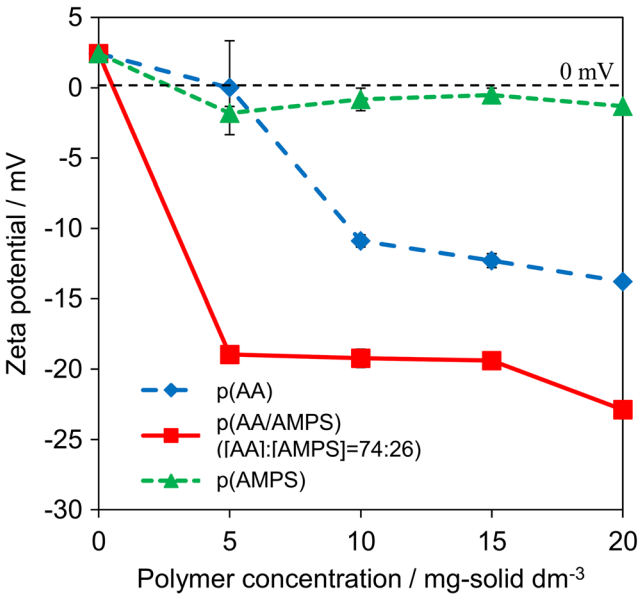

Fig. 6 Zeta potential of the HANCs as a function of the polymer concentration. The zeta potential (mV) in solution was measured using a Zetasizer Nano system after 2 h at 60 °C. *Error bars* show the mean standard deviation after three determinations. No error bars indicate zero or very low mean standard deviation

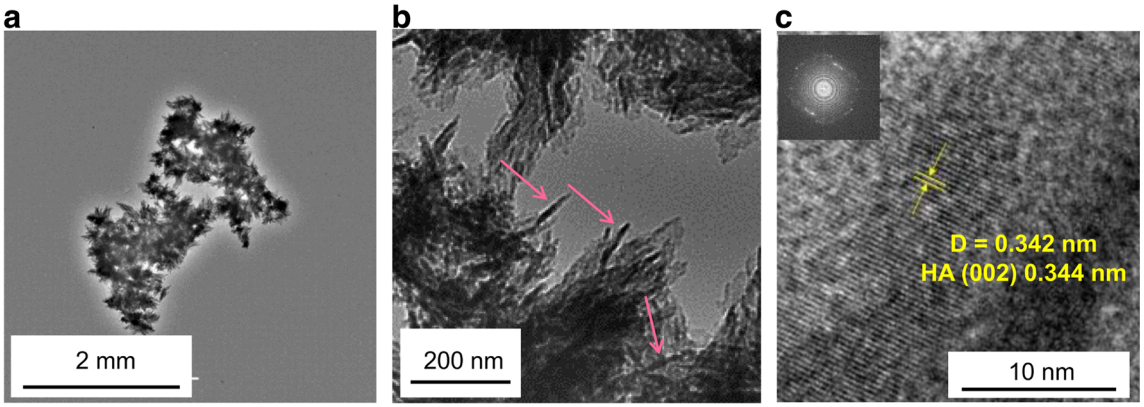

Fig. 7 TEM images of calcium phosphate particles formed with p(AMPS). The insets in (**c**) show the Fourier transforms of the images. Polymer concentration: 20 mg dm^{-3}. The *arrows* indicate the rod-shaped particles of approximately 200 nm length and 10 nm width

of p(AMPS). On the other hand, NC particles were highly dispersed in the presence of p(AA) and p(AA/AMPS) (Figs. 8a and 9a). The lattice fringes of 0.344 and 0.253 nm were assigned to the (002) and (301) planes of HA, respectively [25].

As shown in Figs. 8b, c, and 9b, HANC aggregates of less than 100 nm in size were observed at p(AA) and p(AA/AMPS) concentrations of 20 mg dm^{-3}. The TEM images clearly showed the dispersion of HANCs with a size smaller than 100 nm in those solution where calcium phosphate precipitation was inhibited. When the concentrations of p(AA) and p(AA/AMPS) were 20 mg dm^{-3}, the particle size measured by DLS was below 100 nm. On the other hand, the TEM images also showed the presence of aggregates larger than 100 nm in size. This particles aggregate was suggested to take place during the drying process.

Discussion

Figure 10 shows the elucidated mechanism of nucleation, growth, and dispersion of calcium phosphate particles in the presence of polymers containing carboxy and sulfo groups.

As shown in Fig. 2b, the 0.344 nm lattice spacing observed in the high-resolution TEM image was assigned to the (002) plane of HA [25]. Thus, HANCs approximately 200 nm in size were formed and subsequently aggregated in the supersaturated solution.

As shown in Figs. 7c, 8c, and 9b, lattice fringes of 0.344 and 0.253 nm were assigned to the (002) and (301) planes of HA, respectively [25]. As shown in Figs. 8c and 9b, the particles in solution comprised HANC aggregates of less than 100 nm in size. This result suggested that a nucleus was formed and subsequently grown. Since carboxy groups adsorb on calcium phosphate [17], p(AA) and p(AA/AMPS) containing carboxy groups were expected to adsorb on the surface of the calcium phosphate particles and suppress crystal growth.

From Figs. 3, 5, and 6, it is observed that the dispersibility and negative surface charge of HANCs increased with the p(AA) polymer concentration. Our results implied that the inhibition ability of p(AA) for calcium phosphate precipitation was produced by its large amount of negatively charged carboxy groups. At high polymer concentrations, the amount of carboxy groups not adsorbed on the surface of HANCs increased in the solution. Thus, HANCs were dispersed via

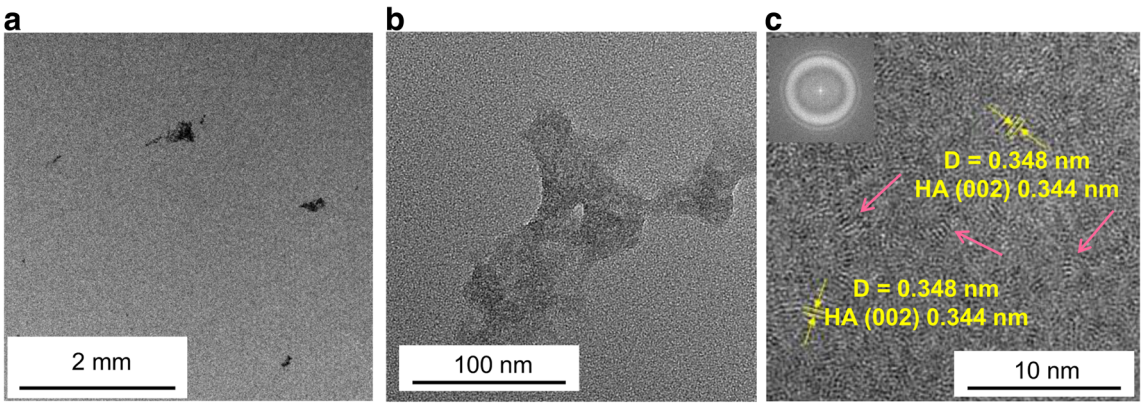

Fig. 8 TEM images of calcium phosphate particles formed with p(AA). Insets in (**c**) show the Fourier transforms of the images. Polymer concentration: 20 mg dm^{-3}. The *arrows* indicate the HA particles

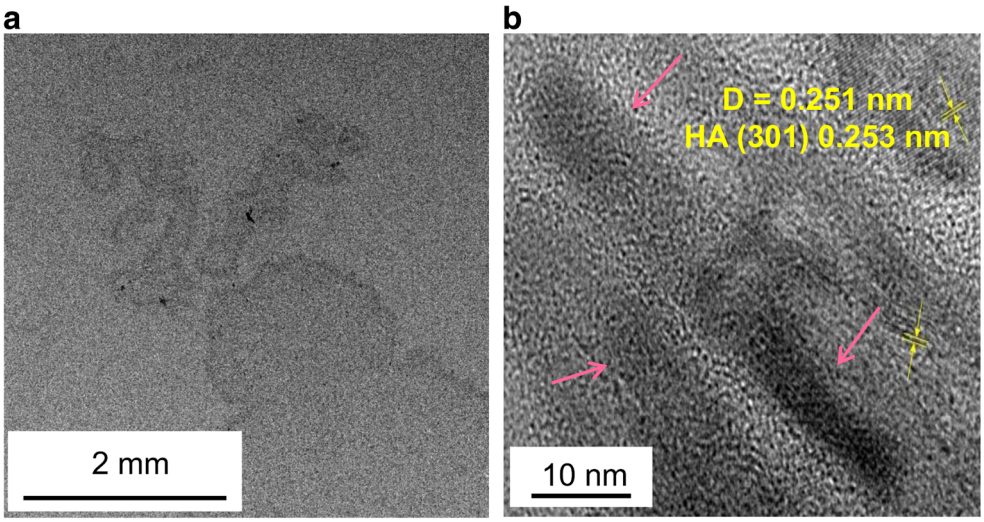

Fig. 9 TEM images of calcium phosphate particles formed with p(AA/AMPS). Polymer concentration: 20 mg dm^{-3}. The *arrows* indicate the HA particles

electrostatic repulsion because of the high amount of carboxy groups and the large negative charge of HANCs.

Figure 5 shows that the HANCs formed with 20 mg dm^{-3} of p(AA/AMPS) were smaller in size as compared to those formed with p(AA). Moreover, as shown in Fig. 6, the zeta potential of the particles generated with p(AA/AMPS) was more negative as compared to p(AA). This suggested that the number of negatively charged groups in p(AA) was lower as compared to p(AA/AMPS). We elucidated the role of sulfo groups in inhibiting calcium phosphate precipitation. Since the pKa values of carboxy and sulfo groups are −4.76 and −1.68, respectively, carboxy and sulfo groups are negatively charged at pH 8.5 [26]. However, at a given concentration, more negatively charged groups are delivered for p(AA/AMPS) as compared to p(AA),

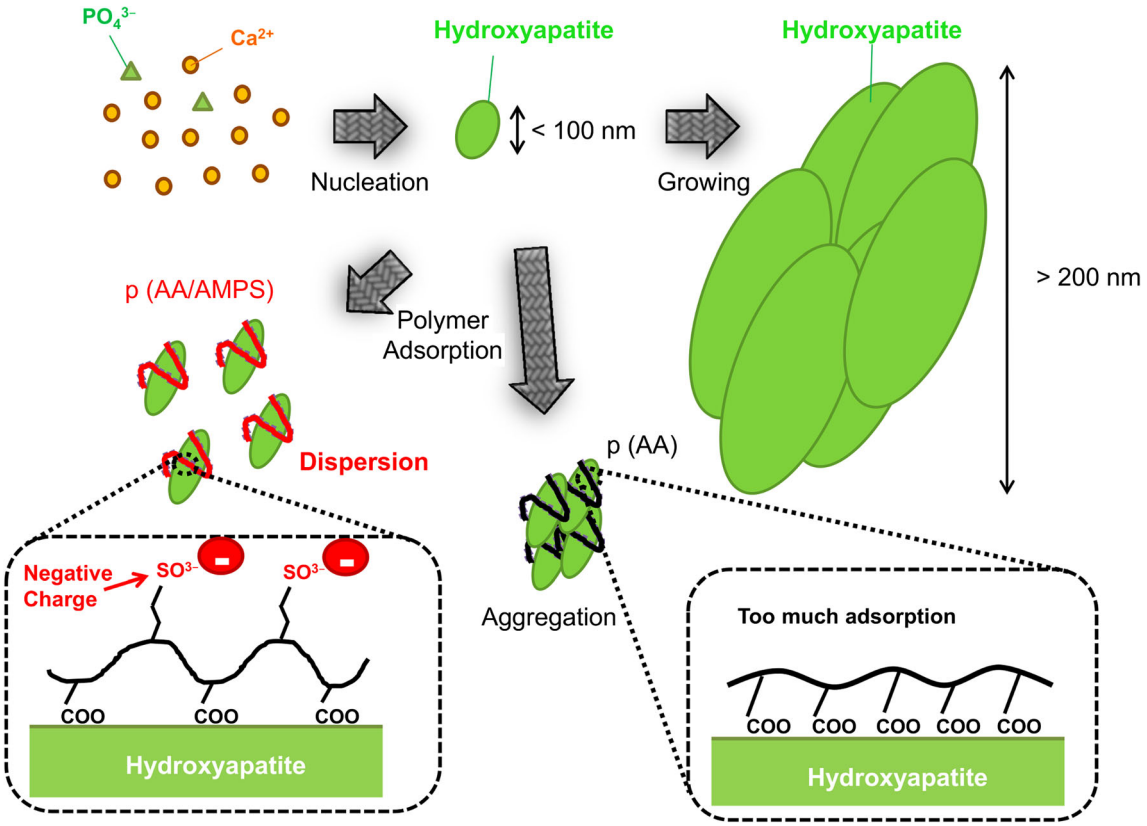

Fig. 10 Dispersion mechanism of calcium phosphate. First, HA nuclei form and grow to a size smaller than 100 nm. Subsequently, p(AA/AMPS) adsorbs onto the nanoparticle surface by binding with the carboxy groups. Sulfo groups of p(AA/AMPS) adsorbed on the HA nanoparticles provide an overall negative charge, resulting in the dispersion of the nanoparticles in solution

because the carboxy groups did not have enough excess negative charge as a result of their strong adsorption on the HANCs. The sulfo groups of p(AA/AMPS), which were adsorbed on calcium phosphate through the carboxy groups, provided an overall negative charge to the HANCs. The dispersion of the HANCs in the supersaturated solution was achieved via electrostatic repulsion. Thus, p(AA/AMPS) exhibited higher precipitation inhibition ability than p(AA). Moreover, p(AA/AMPS) showed high inhibition ability for calcium phosphate precipitation at AA:AMPS ratios of 89:11–24:76. At higher ratios (i.e., higher amounts of carboxy groups) in p(AA/AMPS), there were not enough sulfo groups to disperse the HANCs. On the other hand, at lower ratios (i.e., lower amounts of carboxy groups) in p(AA/AMPS), there were not enough carboxy groups to anchor the p(AA/AMPS) on the HANCs.

Conclusions

Previous investigations have revealed that p(AA/AMPS) containing sulfo groups are effective in inhibiting calcium phosphate scale formation [1, 2, 8]. Moreover, several studies have examined the role of carboxy groups in inhibiting calcium phosphate formation [18, 20]. However, the mechanism by which p(AA/AMPS) inhibits the precipitation of calcium phosphate was not explained in these previous works. Formation and stabilization of HANCs were studied in a supersaturated solution in the presence of copolymers containing carboxy and sulfo groups. We found that the inhibition of calcium phosphate precipitation originates from HANCs with a size smaller than 100 nm in solution. The carboxy groups in the p(AA/AMPS) copolymer adsorbed on calcium phosphate, and the sulfo groups promoted their dispersion by increasing the negative charge of the particles. Future studies can examine the effect of the steric hindrance of sulfo groups on the inhibition ability for calcium phosphate precipitation.

Compliance with ethical standards

Conflict of interest The authors declare that they have no conflict of interest.

Financial funding and support This research received no specific grant from any funding agency in the public, commercial, or not-for-profit sectors.

References

1. Amjad Z (2000) Advances in crystal growth inhibition technologies. In: Amjad Z (ed) Advances in crystal growth inhibition technologies, New York, pp. 71–83
2. Amjad Z (2006) Impact of thermal stability on the performance of polymers as calcium phosphate inhibitors for industrial water systems Phosphorous Res Bull 20:165–170. doi:10.3363/prb.20.165
3. Amjad Z (1988) Effect of precipitation inhibitors on calcium phosphate scale formation Can J Chem 67:850–856
4. Davis VR, Carter WP, Kamrath AM, Johnson AD (1995) The use of modern methods in the development of calcium carbonate inhibitors for cooling water systems. Mineral Scale Formation and Inhibition, New York, pp. 33–46
5. Abdel-Aal N, Satoh K, Sawada K (2002) Study of the adhesion mechanism of $CaCO_3$ using a combined bulk chemistry/QCM technique J Cryst Growth 245:87–100. doi:10.1016/S0022-0248(02)01657-3
6. Sawada K, Abdel-Aal N, Sekino H, Satoh K (2003) Adsorption of inorganic phosphates and organic polyphosphate on calcite Dalton Tran:342–347. doi:10.1039/b209758n
7. Abdel-Aal N, Sawada K (2003) Inhibition of adhesion and precipitation of $CaCO_3$ by aminopolyphosphonate J Cryst Growth 256: 188–200. doi:10.1016/S0022-0248(03)01354-X
8. Amjad Z (1997) Performance of polymers as precipitation inhibitors for calcium phosphate Tenside Surf 34:102–107
9. Amjad Z (2015) Hydroxyapatite dispersion by phosphonates, polymers and phosphonates/polymer blends Phosphorous Res Bull 30: 019–025. doi:10.3363/prb.30.19
10. Urch H, Geismann C, Ulbricht M, Epple M (2006) Synthesis and characterization of DNA-functionalized calcium phosphate nanoparticles Mat-wiss u Werkstofftech 37:422–425. doi:10.1002/mawe.200600008
11. Perkin KK, Turner LJ, Wooley LK, Mann S (2005) Fabrication of hybrid nanocapsules by calcium phosphate mineralization of shell cross-linked polymer micelles and nanocages Nano Lett 5:1457–1461. doi:10.1021/nl050817w
12. Antonietti M, Breulmann M, Goltner GC, Colfen H, Wong WKK, Walsh D, Mann S (1998) Inorganic/organic mesostructures with complex architectures: precipitation of calcium phosphate in the presence of double-hydrophilic block copolymers Chem Eur J 4:2493–2500. doi: 10.1002/(SICI)1521-3765(19981204)4:12<2493::AID-CHEM2493>3.0.CO;2-V
13. Robb DI, Sharples M (1982) The adsorption of poly(acrylic acid) onto insoluble calcium salts J Colloid Interface Sci 89:301–308. doi:10.1016/0021-9797(82) 90182-5
14. Garcia VJ, Carmona P (1982) The effect of some homopolymers on the crystallization of calcium phosphates J Cryst Growth 57:336–342. doi:10.1016/0022-0248(82)90488-2
15. Tay RF, Pashley HD (2008) Guided tissue remineralisation of partially demineralized human dentin Biomaterials 29:1127–1137. doi: 10.1016/j.biomaterials.2007.11.001
16. Peytcheva A, Colfen H, Schnablegger H, Antonitti M (2002) Calcium phosphate colloids with hierarchical structure controlled by polyaspartates Colloid Polym Sci 280:218–227
17. Tsortos A, Nancollas HG (2002) The role of polycarboxylic acids in calcium phosphate mineralization J Colloid Interface Sci 250:159–167. doi:10.1006/jcis.2002.8323
18. Shen X, Tong H, Zhu Z, Wan P, Hu J (2007) A novel approach of homogenous inorganic/organic composites through in situ precipitation in poly-acrylic acid gel Mat Lett 61:629–634. doi:10.1016/j.matlet.2006.05.036
19. Sikiric DM, Milhofer FH (2006) The influence of surface active molecules on the crystallization of biominerals in solution Advan Colloid Interface Sci 128-130:135–158. doi:10.1016/j.cis.2006.11.022
20. Ofir BYP, Govrin-Lippman R, Garti N, Furedi-Milhofer H (2004) The influence of polyelectrolytes on the formation and phase transformation of amorphous calcium phosphate Cryst Growth Des 4: 177–183. doi:10.1021/cg034148g
21. Daniel VK, Dongbo W, Sheng LG (2015) Kinetics of aggregation and crystallization of polyaspartic acid stabilized calcium phosphate particle at high concentrations Biomacromolecules 16: 1550–1555. doi:10.1021/bm501725t

22. Jiang S, Pan H, Chen Y, Xu X, Tang R (2015) Amorphous calcium phosphate phase-mediated crystal nucleation kinetics and pathway Farad Discuss 179:451–461. doi:10.1039/c4fd00212a
23. Yokoi T, Kawashita M, Ohtsuki C (2013) Effects of polymer concentration on the morphology of calcium phosphate crystals formed in polyacrylamide hydrogels J Cryst Growth 383:166–171. doi:10.1016/j.jcrysgro.2013.08.029
24. Demadis DK, Lykoudis P (2005) Chemistry of organophosphonate scale growth inhibitors Bioinorg Chem Appl 3:135–149. doi:10.1155/BCA.2005.135
25. Markovic M, Fowler OB, Tung SM (2004) Preparation and comprehensive characterization of a calcium hydroxyapatite reference materials J Res Natl Inst Stand Technol 109:553–568. doi:10.6028/jres.109.042
26. Guthrie PJ (1978) Hydrolysis of esters of oxy acids: pKa values for strong acids; Bronsted relationship for attack of water at methyl; free energies of hydrolysis of esters of oxy acids; and a linear relationship between free energy of hydrolysis and p*K*a holding over a range of 20 pK units Can J Chem 56:2342–2354